High Sensitive Long Period Fiber Grating Biosensor for Cancer Biomarker Detection

Giuseppe Quero[1], Marco Consales[1], Renato Severino[1], Patrizio Vaiano[1], Alessandra Boniello[1], Annamaria Sandomenico[2], Menotti Ruvo[2], Anna Borriello[3], Laura Diodato[3], Simona Zuppolini[3], Michele Giordano[3], Immacolata Cristina Nettore[4], Annamaria Colao[4], Paolo Emidio Macchia[4], Flavio Santorelli[5], Antonello Cutolo[1] and Andrea Cusano[1]

[1]*Optoelectronics Group, Dept. of Engineering, University of Sannio, Benevento, Italy*
[2]*Istituto di Biostrutture e Bioimmagini, Consiglio Nazionale delle Ricerche (IBB-CNR) and Centro Interuniversitario di Ricerca sui Peptidi Bioattivi (CIRPeB), Napoli, Italy*
[3]*Institute for Polymers, Composites and Biomaterials (IPCB) -CNR, Portici, Italy*
[4]*Department of Clinical Medicine and Surgery, University of Napoli "Federico II", Napoli, Italy*
[5]*Hospital Consulting SpA, Bagno a Ripoli, Firenze, Italy*

Keywords: Long Period Fiber Grating (LPG), Optical Fiber Biosensor, Reflection Type LPG, Thyroglobulin.

Abstract: We report an innovative fiber optic biosensor based on Long Period Gratings (LPGs) working in reflection configuration for real time monitoring of human Thyroglobulin (Tg), a protein marker of differentiated thyroid cancer. A standard LPG is first transformed in a practical probe working in reflection mode, and then it is coated with a single layer of atactic polystyrene (aPS) in order to increase its surrounding refractive index sensitivity and to provide, at the same time, the desired interfacial properties for a stable anti-Tg antibody. The functionalized reflection-type LPG biosensor clearly demonstrates the effectiveness and sensitivity of the developed biosensing platform, allowing the real time and label-free detection of Tg in the needle washouts of fine-needle aspiration biopsies, at concentrations useful for pre- and post-operative assessment of the biomarker levels. Analyte recognition and capture were confirmed with a parallel on fiber ELISA-like assay using, in pilot tests, the biotinylated protein and HRP-labeled streptavidin for its detection. Dose-dependent experiments showed that the detection is linearly dependent on concentration within the range between 0 and 4 ng/mL, while antibody saturation occurs for higher protein levels.

1 INTRODUCTION

The ever increasing incidence of cancer diseases is imposing the development of highly sensitive and effective tools for the real-time detection of associated biomarkers for early diagnosis and optimal treatment. This is particularly needed for the diagnosis of papillary thyroid cancer, whose incidence has dramatically increased over the past few years in the United States and is predicted to increase in the next years, recording a greater frequency in the female population (Weir et al., 2015). Papillary thyroid cancer is the most common malignancy of the thyroid. Although it has favorable long-term outcome, an early stage diagnosis is fundamental to reduce morbidity and mortality. The frequency of lymph nodes involvement is 27% to 46% at initial diagnosis and the recurrence rate is 3% to 30% during post-operative follow-up. Distinguishing lymph nodes metastasis from benign reactive lymphadenitis is therefore critical to rank the malignancy risks in patients with papillary thyroid cancer (Moon et al., 2013).

Thyroglobulin (Tg) is a thyroid specific 660 kDa dimeric protein used by thyroid follicular cells as precursor for biosynthesis of thyroid hormones. Serum Tg levels are elevated in patients with goiter and in several other clinical conditions, and to date, the measurement of Tg is the mainstay in the post-surgical follow-up of differentiated thyroid cancer

Quero, G., Consales, M., Severino, R., Vaiano, P., Boniello, A., Sandomenico, A., Ruvo, M., Borriello, A., Diodato, L., Zuppolini, S., Giordano, M., Nettore, I., Colao, A., Macchia, P., Santorelli, F., Cutolo, A. and Cusano, A.
High Sensitive Long Period Fiber Grating Biosensor for Cancer Biomarker Detection.
DOI: 10.5220/0005846705610569
In *Proceedings of the 9th International Joint Conference on Biomedical Engineering Systems and Technologies (BIOSTEC 2016) - Volume 5: HEALTHINF*, pages 561-569
ISBN: 978-989-758-170-0

(Pacini and Pinchera, 1999), As thyroid-specific protein, its levels in lymph nodes are normally very low and an increased Tg level in the needle washout has been associated with metastasis of lymph nodes in patients affected by differentiated thyroid carcinoma (Giovanella et al., 2013). Its determination is currently based on immunometric-chemiluminescent or radioimmunometric assays (Spencer and Lopresti, 2008).

In recent years, efforts to define and optimize diagnostic and biosensing tools that incorporate such features are significantly increased. Molecular biosensors are preferred as clinical diagnostic tools than other traditional methods because of real-time measurement, rapid diagnosis, multi-target analyses, automation, and reduced costs. A few works have so far been proposed regarding Tg detection using a biosensor platform. In 2008 Choi et al. detected Tg in a cocktailed mixture of proteins by using the competitive protein adsorption/exchange reactions, namely Vroman effect. Implemented on a microfluidic system, the target protein displaced a pre-adsorbed weak-affinity protein on one surface of the device, while another pre-adsorbed high-affinity protein on an adjacent surface was not displaced. Differential measurement using surface plasmon resonance (SPR) phenomenon allowed Tg detection (Choi and Chae, 2009). Recently Dantham et al. (Dantham et al., 2013) reported the detection of single human Tg protein molecule from the resonance frequency shift of a whispering gallery mode-nanoshell hybrid resonator upon adsorption on the nanoshell. However, although the high sensitivity of the proposed devices, the absence of a bioreceptor featuring high specificity and affinity, which can then discriminate between target and non-target molecules, prevented the use of such systems in clinical and diagnostic applications.

Moreover in the last years, the continuous demand for lower limits of detection combined with cost effectiveness and reliability features has been the driving force for the successful demonstration of optical label free biosensors with impressive figures of merit (Fan et al., 2008; Hoa et al., 2007). Relative principles of operation include SPR (Chung et al., 2006; Teramura and Iwata, 2007), interferometry (Weisser et al., 1999; Schneider et al., 1997), optical waveguide-based biosensors (Website, http:// www.neosensors.com), optical ring resonators (Chao et al., 2006; Ren et al., 2007; Hanumegowda et al., 2005), fiber-based biosensors (Lee and Fauchet, 2007; Skivesen et al., 2007; Chryssis et al., 2005; DeLisa et al., 2000; Zhang et al., 2005). Among the others, fiber optic optrodes constitute a valuable platform for label biosensing because of its intrinsic biocompatibility, compact size, multiplexing capability, remote operation and easy integration in medical needles. In particular, in this work we selected optical fiber LPGs as evanescent wave-based biosensors for the measurements of local refractive changes due to molecular binding occurring at the sensor surface (Pilla et al., 2011; Pilla et al., 2012, Del Villar et al., 2005; Cusano et al., 2006, Pilla et al., 2009).

An LPG consists of a periodic modulation of the refractive index (RI) at the core of an optical fiber that results in the coupling of the light between core and cladding modes (James and Tatam, 2003). Thanks to the giant sensitivity to surrounding refractive index (SRI) changes, LPGs represent a very promising technological platform, which can be employed in a wide number of chemical and biological applications (Chiavaioli et al., 2014; Eftimov, 2010; Baldini et al., 2012; Tripathi et al., 2012; Smietana et al., 2015; Falciai et al., 2001; Falate et al., 2005; Chen et al., 2007; Ramachandran et al., 2002).

One of the peculiarities of LPGs platforms is their operation in transmission mode which makes the device sensitive to the bending, therefore requiring the development of appropriate strain-free packages to host the LPG device. In particular, the bending applied on the LPG can introduce unexpected variations in the spectrum of the transmitted optical signal, thus complicating the sensor signal interpretation. In addition the capability to work in reflection mode addresses the mentioned issues and allows the easy integration of the reflective optrode in the vials containing the biological solution and represents a more practical and robust solution to be employed for concrete biological applications (Huang et al., 2013; Quero et al., 2015; Alwis et al., 2013; Cao et al., 2013).

In this work, we present the development of a reflection-type LPG biosensor able to perform the real time detection of thyroid cancer biomarkers in the needle washouts of fine-needle aspiration biopsies. After fabrication, the reflection-type LPG is functionalized with a hydrophobic coating of a specific bioreceptor, in our case an anti-Tg monoclonal antibody and the protein is detected in label-free experiments. Results clearly demonstrate the effectiveness and sensibility of the biosensing platform, allowing the in vitro detection of sub ng/ml concentrations of human purified Tg. To validate the potential translation of such LPG-based biosensor into the clinical practice, detection experiments on clinical samples have been carried out.

2 FABRICATION PROCESS

2.1 Reflection-type LPG Transducer Fabrication

A customized LPG (Λ=370μm) UV-written in a standard single-fiber was used for the biosensor fabrication. To realize a more practical probe which has to be immersed into laboratory vials containing the biological samples under test, the crucial step is the development of an LPG working in reflection configuration. The first steps regarding the fabrication of the reflection-type LPG (RT-LPG) probe is the cut of the fiber inside which the LPG is inscribed and the integration of a completely reflecting layer (i.e. a mirror) on the fiber facet (see Figure 1). A key aspect of this step is the identification of the precise LPG position within the fiber. This is of primary importance in order to cut the fiber just after the grating, and to avoid the formation of interference fringes within the attenuation bands, typical of self-interfering LPGs (Alwis et al., 2013).

Once identified the LPG position, a high precision fiber cleaver (Fujikura CT-30) was used to cut the optical fiber just after the grating, followed by the integration of an Ag reflecting layer on the facet of the cut fiber. To this aim, a silver mirror reaction (Tollen's test) was adopted (Yin et al., 2002).

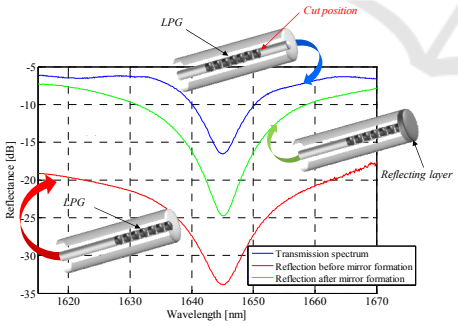

Figure 1: LPG spectra acquired in air before the fiber cut (blue curve), just after the fiber cut (red curve) and after the mirror integration (green curve) and schematics of the reflection-type LPG fabrication steps (in the insets).

Figure 1 shows the LPG spectra acquired just before the optical fiber cut (i.e. in transmission configuration), after the fiber cut (i.e. in reflectance configuration before the mirror formation) and after the mirror formation at the fiber end-face. It can be seen that a significant baseline reduction occurs after the cut (red curve), mainly due to the fact that light passing through the LPG is mostly transmitted at the fiber/air interface, and only a small portion (~3-4%) of it is reflected back into the fiber. Nevertheless, as soon as the Ag layer is formed at the fiber termination, almost all the initial power is recovered (green curve). We point out that the use of reflection-type LPGs not only is of fundamental importance to transform an LPG-based sensor in a more practical probe for concrete biomedical applications, but also improves the resonance visibility (see Figure 1) due to the double passing of light through the grating.

2.2 Overlay Deposition

The last fabrication step relied on the aPS overlay deposition onto the RT-LPG surface using the dip-coating (DC) technique. In particular, the aPS overlay deposition was performed via the DC process by means of an automated system (NIMA Technology Micro-Processor Interface IU 4) at an immersion/extraction speed of 100 mm/min (Pilla et al., 2011; Pilla et al., 2009).

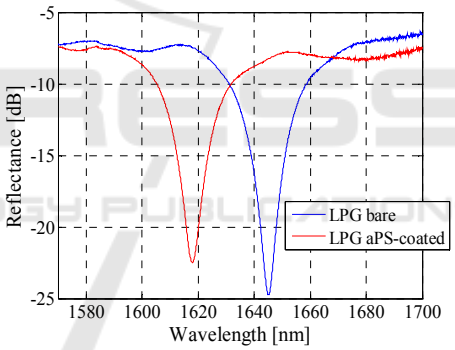

Figure 2: Spectra of the bare (blue line) and aPS-coated (red line) RT-LPG.

Figure 2 reports the spectral position of the sixth order cladding mode in the bare RT-LPG (blue curve) and after the aPS overlay deposition (red curve). All the spectra were recorded with the device surrounded by air.

The aPS overlay thickness was chosen on the basis of a preventive design process (carried out by means of a virtual environment for the analysis and simulation of nano-scale coated LPGs) in order to optimize the device sensitivity in correspondence of an SRI=1.340, which approaches the RI of the buffer solution used in our binding experiments. The optimized thickness overlay allows the modal transition phenomena to take place and makes the reflection-type LPG very high sensitive for a SRI=1.340 is 310 nm.

The spectral characterization of the fabricated LPG versus SRI has been carried out by submerging the probe into aqueous glycerol solutions characterized by different RI in the range 1.335-1.460, in order to validate the fabrication process success and the SRI sensitivity in correspondence of an SRI=1.340. To this aim, an optoelectronic set-up (see Figure 3) comprising a broadband light source (with bandwidth 1200-1700 nm), a 2x1 directional coupler and an optical spectrum analyzer (OSA, ANDO AQ6317C, wavelength resolution 10 pm, dynamic range 60 dB) was used for the acquisition of the LPG reflection spectrum at the different stages of the device fabrication and characterization. The OSA is connected to a personal computer and controlled by a LabView plug-in, enabling the automatic acquisition of the RT-LPG spectra. Acquired spectra are then automatically filtered and elaborated by a MATLAB script that provides the central resonance wavelengths (λc) of each spectrum.

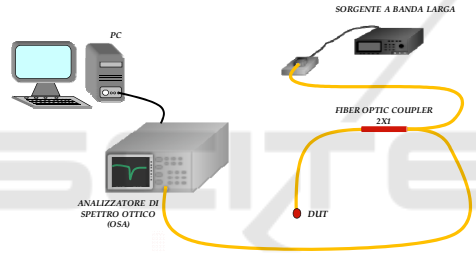

Figure 3: Schematic interrogation set-up.

During the biological experiments the RT-LPG spectra is automatically acquired every 45 seconds, thus providing a continuous and real time monitoring of the interaction kinetics of the biological molecules on the RT-LPG surface.

2.3 Surrounding Refractive Index (SRI) Sensitivity Characterization

The spectral characterization of the fabricated LPG versus SRI has been carried out by submerging the probe into aqueous glycerol solutions characterized by different RI in the range 1.335-1.460.

As reported in Figure 4b, the obtained SRI sensitivity (|∂λc/∂SRI|) exhibits the typical resonance-shaped behavior of transition mode LPG, thus confirming the fabrication process success. At the same time, it can be seen that the SRI sensitivity in correspondence of an SRI=1.340 is equals to ~1700 nm/RIU.

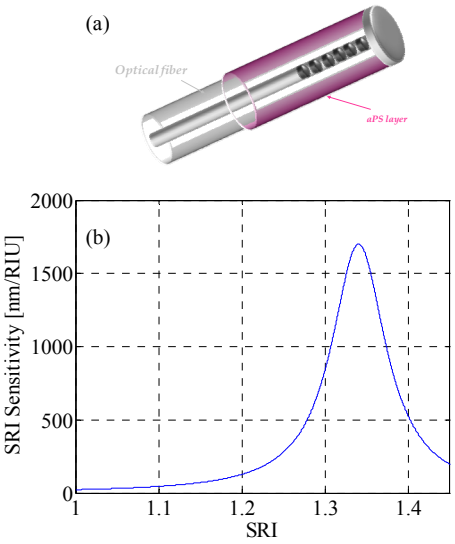

Figure 4: a) Schematic view of the final RT-LPG transducer and b) Experimental SRI sensitivity (|∂λc/∂SRI|) vs. SRI curve for the cladding mode LP_{07}.

3 CHARACTERIZATION OF THE TG/ANTI-TG MAB INTERACTION

As a Tg bioreceptor we choose one of the several commercially available anti-Tg monoclonal antibodies because such reagents are generally characterized by extremely high specificity and affinity for the target molecules. The affinity of the monoclonal antibody for Tg was however assessed using both traditional immunoenzymatic and real-time assays. An indirect ELISA was firstly performed by adsorbing Tg on multiwell plates and adding increasing amounts of the mouse anti-Tg monoclonal antibody (Figure 5a). Following the detection step with an anti-mouse antibody conjugated with HRP, increasing chromogenic signals (corresponding to increased bound analyte) were recorded with increasing antibody concentration. As shown in Figure 5a, a strong and saturable binding signal was observed even at low antibody concentrations. Saturation started at 100 pM mAb. Fitting of data points by a non-linear algorithm, where we assumed a 1:1 binding stoichiometry, provided a Dissociation constant (KD) of 72 pM, a value indicative of the high affinity of the antibody for the specific analyte. The presence of high concentrations of BSA in the assay (1% w/w, that is 10 mg/mL), also provided a very strong indication of selectivity. Indeed blank signals

were negligible and after subtraction a 2.0 AU residual signal was measured at saturation. To further characterize the binding between the antibody and Tg, we next performed a label free binding assay using an SPR-based instrument (BIAcore). The anti-Tg antibody and Tg were thereby immobilized on the surface of the sensor chip (1120 and 650 RU immobilization level, respectively. Not shown). In one experiment with the Tg-derivatized chip, mAb solutions at increasing concentrations, between 0.25 and 1.5 nM, were injected.

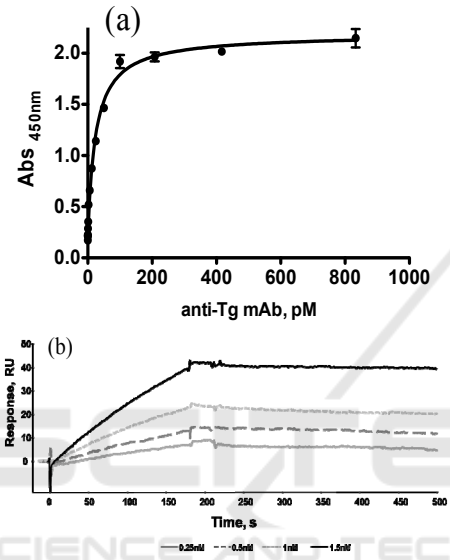

Figure 5: Biochemical system characterization. a) Dose-response indirect ELISA assay performed to assess antigen/antibody affinity. b) SPR assay using Biacore of the binding kinetic of anti-Tg monoclonal antibody to immobilized Tg, at different antibody concentrations.

As shown in Figure 5b, dose-response association and dissociation curves were obtained witnessing the high affinity and specificity of the interaction. Using the kinetic parameters a KD of 70 pM was estimated. This value was in full agreement with that extrapolated by ELISA, confirming the strength of the interaction and the high specificity. When we probed the immobilized antibody with soluble Tg a significantly higher KD (about 1.3 nM) was determined (data not shown) than that determined by ELISA. This was likely due to inappropriate antibody immobilization.

3.1 Assessment of Tg Capture on LPG Biosensor Surface by on-Fiber ELISA-like Assay

Figure 6a shows a typical sensorgram, reporting the measured resonance wavelenghts as function of time, observed for a biotinylated human Thyroglobulin detection assay and in the inset the magnification of the experiment final step regarding the Tg detection.

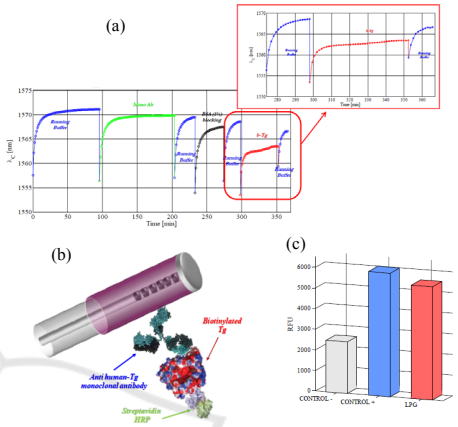

Figure 6: a) Sensorgram obtained for the detection of 40µg/ml biotinylated human Thyroglobulin using the reflection-type Long Period Grating biosensing platform; b) schematic view of the ELISA-like assay performed on the functionalized LPG; c) binding signals obtained by the ELISA-like assay.

After a prolonged and satisfactory adaptation of the functionalized biosensor in the running buffer, an anti-Thyroglobulin monoclonal antibody, previously selected for its affinity and specificity for the identified marker and deeply characterized by label-free and immunoenzymatic assays, was immobilized on the probe active surface via hydrophobic coating, recording a 1.9 nm wavelength shift of the resonant peak.

After analyte capture to the specific receptor (see magnification in Figure 6a, a 2.0 nm wavelength shift of the resonant peak was observed. To avoid the influence of the different solutions refractive index change, peak shifts have been estimated as a difference between two successive immersions in the running buffer, specifically before and after dipping the sensor in the test solution. In addition, by exploiting the binding of HRP-labeled streptavidin to the biotinylated Thyroglobulin, analyte capture was confirmed in a parallel on fiber ELISA-like assay (Figure 6b-c).

4 DETECTION OF TG WITH LPG BIOSENSOR

4.1 Calibration Curve for the Detection of Human Tg with LPG Biosensor

To use the platform for the detection of Tg in biological fluids, we first evaluated the system dose-response features and the associated sensitivity. The system was therefore tested on a set of several different Tg solutions at different concentrations ranging between 0.08 ng/mL (0.13 pM) to 88 ng/mL (146 pM). Since no regeneration steps were carried out, different LPG biosensors were used for this test and each transducer was used for the detection of two cumulative and consecutive analyte concentrations.

At the different concentrations (0.08 ng/mL, 0.88 ng/mL, 4.0 ng/mL, 8.0 ng/mL, 44 ng/mL and 88 ng/mL), we observed the following average values of $\Delta\lambda_{Tg\text{-}binding}$: 0.26 nm, 1.03 nm, 1.65 nm, 2.45 nm, 3.35 nm and 3.58 nm, respectively. A blank average value of 0.10 nm, accounting for the non-specific binding, was instead measured using the transducer without antibody coating. The corresponding dose-dependent curve is reported in Figure 7, where we can observe the dose-dependency and the saturation reached yet between about 20 and 30 ng/mL of Tg (33 pM and 50 pM, respectively). Also, the analyte could be still detected with a remarkable difference over the non-specific recognition at the lowest concentration of 0.08 ng/mL.

Although the fabrication process was robust and repeatable, a normalization procedure was needed to account for the even tiny differences of device performances. Such differences may occur due to the LPG fabrication tolerances, or to slightly different antibody coatings obtained on the distinct devices. To normalize the signals we used the wavelength shift occurred upon mAb coating, as an indirect measure of surface sensitivity of each LPG probe. We thus calculated the final observable (O) as reported in the following equation 1:

$$\text{Observable (O)} = \Delta\lambda_{Tg\text{-}binding} + \Delta\lambda_{mAb\text{-}coating} \quad (1)$$

Where, $\Delta\lambda_{Tg\text{-}binding}$ and $\Delta\lambda_{mAb\text{-}coating}$ are the differences between the stabilized central wavelength of the attenuation band in buffer solutions before and after contact with the biomolecule solution and denote Tg binding and mAb coating onto the LPG surface, respectively. The KD was determined by reporting the observed resonance peak shift at every concentration versus analyte concentration. Some antibody-coated optical fibers were immersed in buffer alone and used as blank.

Hydrophobic adsorption of the antibody can be influenced by several factors, such as temperature, exposure time, different surface properties and ligand orientation, thus influencing transducer sensitivity. Such variability could result in different effective detection capability and sensitivity between different functionalized biosensors. Moreover, any sensitivity variation of the biosensor associated to different polymer thickness, that could cause significant underestimation of Tg concentration, is in this way corrected. It is also important to underscore that the dip-coating technique used to deposit the polymer on the optical fibers, does not guarantee a tight control over polymer thickness at the nanometer scale. The normalization that we have introduced attenuates the impact of such factors and we indeed observed an optimal correlation between data obtained with different optical fibers.

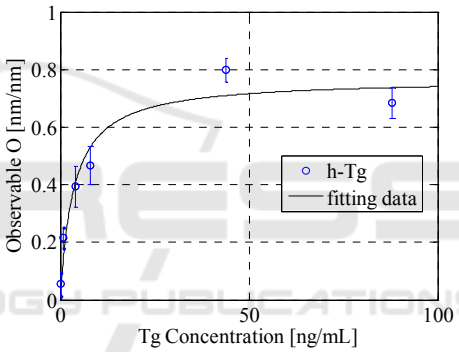

Figure 7: Calibration curve for the semi-quantitative detection of human Thyroglobulin using RT-LPG biosensor. Blue dots refer to the dose-dependent assay performed to obtain the calibration curve.

Data clearly show that human Tg bound with high affinity and in a dose dependent manner to the monoclonal antibody immobilized onto the solid phase. Also, it is worth noting that the level of nonspecific adsorption of analyte to the surface is particularly low, suggesting that functionalization and blocking were particularly effective and that selectivity was also particularly high, given the very poor recognition of albumin present at high concentration.

From the plot of resonance peak shifts against analyte concentration reported in Figure 7, we also estimated a KD of about 6 pM, which is in the same low pM range of that determined by ELISA and by Biacore (about 70 pM). Such KD value also reflects the high sensitivity of the detection system, which is able to detect as low as 0.08 ng/mL Tg under these

conditions. A linear dose-response is grossly obtained within the 0 – 4 ng/mL range (0 – 6.7 pM).

4.2 Detection of Tg in Clinical Samples

RT-LPG-based biosensors were used for the ex-vivo detection of human Tg from needle washouts of fine-needle aspiration biopsies of thyroid nodules from several different patients.

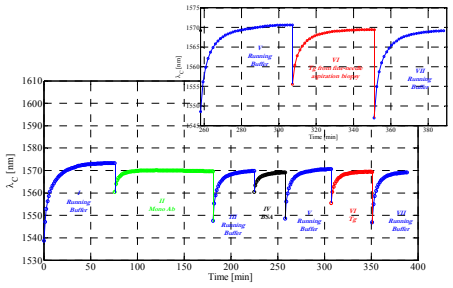

Figure 8: RT-LPG sensorgram reporting the wavelength shift of 6th order cladding mode attenuation band during human Thyrogobulin detection from the needle washout of fine-needle aspiration biopsy. In magnification the wavelength shift during Thyroglobulin binding event is reported.

Figure 8 shows typical sensorgrams obtained for such the real-time detection of human Tg. The transducer was functionalized as described above by immersing the probe in a solution containing the anti-Tg mAb. After the blocking step necessary to reduce non-specific adsorption of the analyte, the probe was immersed in solutions obtained by diluting the needle washout of fine-needle aspiration biopsies (steps V-VII in the magnification). Such solutions contained Tg at different concentrations, previously quantified using a standard immunoenzymatic assay. Different independent assays were performed with solution samples at increasing Tg concentrations, observing a remarkable correlation with the calibration curve previously obtained (Figure 9, red dots) and with the concentrations obtained by canonical Tg quantification. In particular, a first set of human samples was diluted at 1 ng/mL Tg (within the linearly responsive range) and detection was performed with different RT-LPG biosensors. As shown in Figure 9, we obtained an average value for the observable O of 0.225 corresponding to 1.45 ng/mL Tg, a value in very good agreement with the expected concentration. An independent detection assays were performed on human samples prepared at 5 ng/mL Tg, obtaining average O values of 0.430, corresponding to 4.5 ng/mL. Also in this case values were in an overall satisfactory agreement with those expected, confirming the linear dose-response within the expected range and, most importantly, the substantial lack of strong non-specific interactions with other high concentration plasma proteins that contaminate the washout samples. Finally, the detection assays were performed on undiluted samples, coming from different patient specimens, having Tg concentrations higher than 3000 ng/mL. The average O values obtained after Tg capture were 0.777, corresponding, as expected, to complete biosensor saturation. We reported the values on the plot of Figure 9 as red dots after the dashed line to underline the substantial accordance between Tg detection with LPG biosensors and canonical immunoenzymatic techniques.

Such reference values clearly indicate that the biosensor operates at best in a range of concentrations matching that having a high clinical relevance.

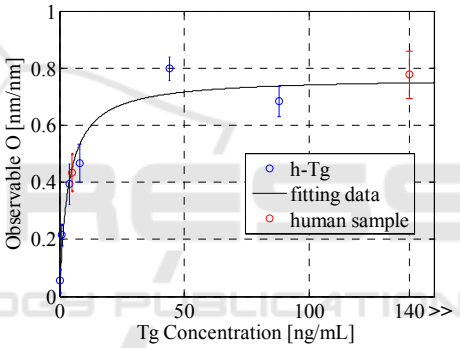

Figure 9: Calibration curve for the semi-quantitative detection of human Thyroglobulin using RT-LPG biosensor and ex-vivo detection of human Thyroglobulin from needle washout of fine-needle aspiration biopsy. Blue dots refer to the dose-dependent assay performed to obtain the calibration curve, while red dots refer to the ex-vivo assay performed on human samples. The response is roughly linear within the range 0 – 4 ng/mL.

In order to improve prognosis of differentiated thyroid carcinomas, it is widely accepted that confirmed or suspected cervical Lymph Nodes (LN) metastases should be removed for local control. However either preoperatively with ultrasonography (US) or during the operation, it is difficult to recognize small and occult LN metastases in the central compartment (Chéreau et al., 2015). Although it is widely accepted that differentiated thyroid carcinoma recurrences after lymph node dissection is unrelated to the number of LNs removed (Albuja-Cruz et al., 2012), it is also well established that removing occult LN metastasis decreases the rate of recurrence in the neck (Roh et

al., 2011). The clinical application of real time Tg detection will probably in a near future provide to surgeons a powerful and reliable tool to precisely identify metastatic lymph nodes.

5 CONCLUSIONS

We report an innovative fiber optic nano-optrode based on LPGs working in reflection mode for real time monitoring of human Thyroglobulin, a protein marker of differentiated thyroid cancer.

The reflection-type LPG biosensor, coated with a single layer of atactic polystyrene onto which a specific, high affinity anti-Tg antibody was adsorbed, allowed the real time and label-free detection of Tg in the needle washouts of fine-needle aspiration biopsies, at concentrations useful for pre- and post-operative assessment of the biomarker levels.

Analyte recognition and capture were confirmed with a parallel on fiber ELISA-like assay using, in pilot tests, the biotinylated protein and HRP-labeled streptavidin for its detection. Dose-dependent experiments showed that the detection is linearly dependent on concentration within the range between 0 and 4 ng/mL, while antibody saturation occurs for higher protein levels. The system is characterized by a very high sensitivity and specificity, which reflects the specificity and affinity of the antibody chosen as capturing bioreceptor. Indeed, the biosensor allowed the ex-vivo detection of sub ng/ml concentrations of human Tg from needle washouts of fine-needle aspiration biopsies of thyroid nodule from different patients.

Data here presented underline the high potential of the proposed biosensing platform and the several advantages of this kind of transducer: the absence of labeling requirements represents in fact an attractive alternative to traditional label-based techniques such as fluorescence, colorimetry or radioactivity-based approaches, without affecting the intrinsic affinity. Furthermore, it appears particularly useful for monitoring post-operative Tg levels, as the Tg warning concentration (about 1 ng/mL) is well within our linear response range (about 0 – 4 ng/mL). We foresee that, following a further optimization and standardization of the detection protocol, such an application is close at hand under the current experimental settings. We also believe that a further engineering of the detection platform could allow the detection of Tg during biopsy collection. However this would require suitable needles and proper microfluidic and washing devices for the removal of tissue debris and for analyte dilution, a step strongly needed in light of the very high sensitivity of the detection system.

Although the detection times are still in the hour range, we do believe that the integration with a microfluidic system will significantly reduce the response time, making this method time saving, an essential parameter for its application in the clinical field. In addition a multiplexed configuration, with the parallel detection of several biomarkers of clinical interest, appears as a possible future target.

ACKNOWLEDGEMENTS

The authors gratefully acknowledge the financial support from the national project “Smart Health 2.0”, funded by the Italian Ministry of Education, University and Research (MIUR) under the PON framework.

REFERENCES

Albuja-Cruz, M. B., Thorson, C. M., Allan. B. J., Lew. J. I., Rodgers. 2012, Surgery, 152, 1177–1183.

Alwis, L., Sun, T., Grattan, K. T. V., 2013. *Sens. Actuators*, B, 178, 694–699.

Baldini, F., Brenci, M., Chiavaioli, F., Giannetti, A.,Trono, C., 2012. *Anal. Bioanal. Chem*. 402, 109–116.

Cao, J., Tu, M. H., Sun, T., Grattan, K. T. V., 2013. Sens. Actuators, B, 181, 611–619.

Chao, C. Y., Fung, W., Guo, L. J., 2006. IEEE J. Sel. Top. *Quantum Electron*. 12, 134-142.

Chen, X., Zhou, K., Zhang, L., Bennion, I., 2007. *Appl. Opt*. 46, 451–455.

Chéreau, N., Buffet, C., Trésallet, C., Tissier, F., Leenhardt, L., Menegaux, F. 2015. Surgery. 15, 704-707.

Chiavaioli, F., Biswas, P., Trono, C., Bandyopadhyay, S., Giannetti, A., Tombelli, S., Basumallick, N., Dasgupta, K., Baldini, F., 2014. *Biosens. Bioelectron*. 60, 305–310.

Choi, S., Chae, J., 2009. *Biosens. Bioelectron*. 25, 118–123.

Chryssis, A. N., Saini, S.S., Lee, S. M., H. Yi, Bentley, W.E., Dagenais, M., 2005. IEEE J. Sel. Top. *Quantum Electron*. 11, 864-872.

Chung, J. W., Bernhardt, R., Pyun, J. C., 2006. *Sens. Actuators B Chem*. 118, 28-32.

Cusano A., Iadicicco, A., Pilla, P., Contessa, L., Campopiano, S., Cutolo, A., Giordano, M., 2006a. Opt. Express, 14, 19–34.

Dantham, V. R., Holler, S., Barbre, C., Keng, D., Kolchenko, V., Arnold, S., 2013. *Nano Lett*. 13, 3347-3351.

DeLisa, M. P., Zhang, Z., Shiloach, M., Pilevar, S., Davis, C.C., Sirkis, J.S., Bentley, W.E., 2000. *Anal. Chem*. 72, 2895–900.

Del Villar, I., Matías, I. R., Arregui, F. J., Lalanne, P., 2005. Opt. Express, 13, 56–69.

Eftimov, T., 2010. Applications of Fiber Gratings in Chemical and Biochemical Sensing, in: *Zourob, M., Lakhtakia, A. (Eds.), Optical Guided-wave Chemical and Biosensors II, Springer Series on Chemical Sensors and Biosensors 8, Springer Berlin, Heidelberg*, pp. 151–176.

Falate, R., Kamikawachi, R. C., Müller, M., Kalinowski, H. J., Fabris, J. L., 2005. *Sens. Actuators B Chem*. 105, 430–436.

Falciai, R., Mignani, A.G., Vannini, A., 2001. *Sens. Actuators B Chem*. 74, 74–77.

Fan, X., White, I. M., Shopova, S. I., Zhu, H., Suter, J. D., Sun, Y., 2008. *Anal. Chim. Acta*. 620, 8-26.

Garg, R., Tripathi, S. M., Thyagarajan, K., Bock, W. J., 2013. Sens. Actuators, B, 176, 1121–1127.

Giovanella, L., Bongiovanni, M., Trimboli, P., 2013. *Curr Opin Oncol*., 25: 6-13.

Hanumegowda, N.M., White, I.M., Oveys, H., Fan, X., 2005. *Sens. Lett*. 3, 315-319.

Hoa, X. D., Kirk, A.G., Tabrizian, M., 2007. *Biosens. Bioelectron*. 23, 15–160.

Huang, J., Lan, X., Kaur, A., Wang, H., Yuan, L., Xiao, H., 2013. *Optical Engeneering*, 52, 014404.

James, S. W., Tatam, R. P., 2003. *Meas. Sci. Technol*. 14, R49–R61.

Lee, M. R., Fauchet, P. M., 2007. *Opt. Express* 15, 4530-4535.

Moon, J. H., Yong I. K., Lim, J. A., Choi, H. S., Cho, S. W., Kim, K. W., Park, H. J., Paeng, J. C., Park, Y. J., Yi, K. H., Park, D. J., Kim, S. E.and .Chung, J. K., 2013. *J Clin Endocrinol Metab*, 98, 1061-1068.

Pacini, F., Pinchera, A., 1999. Biochimie., 81:463-467.

Patrick, H. J., Kersey, A. D., Bucholtz, F., 1998. *J. Lightwave Technol*. 16, 1606–1612.

Pilla, P., Manzillo, P., Malachovská, V., Buosciolo, A., Campopiano, S., Cutolo, A., Ambrosio, L., Giordano, M., Cusano, A., 2009. Opt. Express, 17, 20039–20050.

Pilla, P., Malachovská, V., Borriello, A., Buosciolo, A., Giordano, M., Ambrosio, L., Cutolo, A., Cusano, A., 2011. *Opt. Express*, 19, 512–526.

Pilla, P., Sandomenico, A., Malachovská, V., Borriello, A., Giordano, M., Cutolo, A., Ruvo, M., Cusano, A., 2012. *Biosens. Bioelectron.* 31, 486–491.

Quero, G., Consales, M., Vaiano, P., Cusano, A., Zuppolini, S., Diodato, L., Borriello, A., Giordano, M., Venturelli, A., Costi, M. P., 2015. *XVIII AISEM Annual Conference.*

Ramachandran, S., Wang, Z., Yan, M., 2002. *Opt. Lett*. 27, 698–700.

Ren, H. C., Vollmer, F., Arnold, S., Libchaber, A., 2007. *Opt. Express* 15, 17410-17423.

Roh, J. L., Kim, J. M., Park, C. I. 2011. Ann Surg Oncol, 18, 1312–1318.

Schneider, B. H., Edwards, J. G., Hartman, N. F., 1997. *Clin. Chem*. 43, 1757-1563.

Skivesen, N., Tetu, A., Kristensen, M., Kjems J., Frandsen L. H., Borel P. I, 2007. *Opt. Express* 15, 3169-3176.

Smietana, M., Koba, M., Brzozowska, E., Krogulski, K., Nakonieczny, J., Wachnicki, L., Mikulic, P., Godlewski, M., Bock, W. J., 2015. *Opt. Express*. 23, 8441–8453.

Spencer, C. A., Lopresti, J. S., 2008. *Nature Clinical Practice* 4, 223–233.

Teramura, Y., Iwata, H., 2007. *Anal. Biochem*. 365, 201-207.

Tripathi, S. M., Bock, W. J., Mikulic, P., Chinnappan, R., Ng, A., Tolba, M., Zourob, M., 2012. *Biosens. Bioelectron*. 35, 308–312.

Website, http://www.neosensors.com.

Weir, H. K., Thompson, T. D., Soman, A., Moller, B., Leadbetter, S., 2015. *Cancer*, 121, 1827-1837.

Weisser, M., Tovar, G., Mittler-Neher, Knoll, S. W., Brosinger, F., Freimuth, H., Lacher, M., Ehrfeld, W., 1999. *Biosens. Bioelectron*. 14, 405-411.

Yin, Y., Li, Z. Y., Zhong Z., Gates B., Venkateswaran S., 2002. *S. J. Mater. Chem*. 12, 522−527.

Zhang, Y., Shibru, H., Cooper, K.L., Wang, A., 2005. *Opt. Lett.* 30, 1021–1023.